

Kennesaw State University
DigitalCommons@Kennesaw State University

Faculty Publications

3-2016

Search for the rare decay $D^{\{0\}} \rightarrow \gamma\gamma$ at Belle

N. K. Nisar et al.
Belle Collaboration

D. Joffe
Kennesaw State University, djoffe@kennesaw.edu

Follow this and additional works at: <https://digitalcommons.kennesaw.edu/facpubs>

 Part of the [Physics Commons](#)

Recommended Citation

et al., N. K. Nisar and Joffe, D., "Search for the rare decay $D^{\{0\}} \rightarrow \gamma\gamma$ at Belle" (2016). *Faculty Publications*. 4226.
<https://digitalcommons.kennesaw.edu/facpubs/4226>

This Article is brought to you for free and open access by DigitalCommons@Kennesaw State University. It has been accepted for inclusion in Faculty Publications by an authorized administrator of DigitalCommons@Kennesaw State University. For more information, please contact digitalcommons@kennesaw.edu.



CHORUS

This is the accepted manuscript made available via CHORUS. The article has been published as:

Search for the rare decay $D^{\{0\}} \rightarrow \gamma\gamma$ at Belle

N. K. Nisar *et al.* (Belle Collaboration)

Phys. Rev. D **93**, 051102 — Published 9 March 2016

DOI: [10.1103/PhysRevD.93.051102](https://doi.org/10.1103/PhysRevD.93.051102)

Search for the rare decay $D^0 \rightarrow \gamma\gamma$ at Belle

N. K. Nisar,^{65,1} G. B. Mohanty,⁶⁵ K. Trabelsi,^{15,12} T. Aziz,⁶⁵ A. Abdesselam,⁶⁴ I. Adachi,^{15,12} H. Aihara,⁷¹
 D. M. Asner,⁵³ V. Aulchenko,^{4,51} T. Aushev,^{41,23} R. Ayad,⁶⁴ V. Babu,⁶⁵ I. Badhrees,^{64,28} S. Bahinipati,¹⁷
 E. Barberio,³⁹ P. Behera,¹⁸ V. Bhardwaj,⁶¹ J. Biswal,²⁴ A. Bobrov,^{4,51} A. Bozek,⁴⁸ M. Bračko,^{37,24} F. Breibeck,²¹
 T. E. Browder,¹⁴ D. Červenkov,⁵ V. Chekelian,³⁸ A. Chen,⁴⁵ B. G. Cheon,¹³ R. Chistov,²³ K. Cho,²⁹
 V. Chobanova,³⁸ Y. Choi,⁶² D. Cinabro,⁷⁷ J. Dalseno,^{38,66} N. Dash,¹⁷ Z. Doležal,⁵ Z. Drásal,⁵ A. Drutskoy,^{23,40}
 D. Dutta,⁶⁵ S. Eidelman,^{4,51} H. Farhat,⁷⁷ J. E. Fast,⁵³ B. G. Fulsom,⁵³ V. Gaur,⁶⁵ A. Garmash,^{4,51} R. Gillard,⁷⁷
 Y. M. Goh,¹³ P. Goldenzweig,²⁶ B. Golob,^{34,24} D. Greenwald,⁶⁷ O. Grzymkowska,⁴⁸ J. Haba,^{15,12}
 T. Hara,^{15,12} K. Hayasaka,⁴³ H. Hayashii,⁴⁴ X. H. He,⁵⁵ W.-S. Hou,⁴⁷ K. Inami,⁴² A. Ishikawa,⁶⁹ Y. Iwasaki,¹⁵
 W. W. Jacobs,¹⁹ I. Jaegle,¹⁴ H. B. Jeon,³² D. Joffe,²⁷ K. K. Joo,⁶ T. Julius,³⁹ K. H. Kang,³² E. Kato,⁶⁹
 T. Kawasaki,⁴⁹ C. Kiesling,³⁸ D. Y. Kim,⁶⁰ H. J. Kim,³² K. T. Kim,³⁰ M. J. Kim,³² S. H. Kim,¹³ K. Kinoshita,⁷
 P. Kodyš,⁵ S. Korpar,^{37,24} P. Križan,^{34,24} P. Krokovny,^{4,51} T. Kuhr,³⁵ R. Kumar,⁵⁷ T. Kumita,⁷³ A. Kuzmin,^{4,51}
 Y.-J. Kwon,⁷⁹ I. S. Lee,¹³ J. S. Lange,¹⁰ H. Li,¹⁹ L. Li,⁵⁸ L. Li Gioi,³⁸ J. Libby,¹⁸ D. Liventsev,^{76,15} P. Lukin,^{4,51}
 M. Masuda,⁷⁰ D. Matvienko,^{4,51} K. Miyabayashi,⁴⁴ H. Miyata,⁴⁹ R. Mizuk,^{23,40} S. Mohanty,^{65,75} A. Moll,^{38,66}
 H. K. Moon,³⁰ T. Mori,⁴² R. Mussa,²² E. Nakano,⁵² M. Nakao,^{15,12} T. Nanut,²⁴ Z. Natkaniec,⁴⁸ M. Nayak,¹⁸
 M. Niiyama,³¹ S. Nishida,^{15,12} S. Ogawa,⁶⁸ S. Okuno,²⁵ P. Pakhlov,^{23,40} G. Pakhlova,^{41,23} B. Pal,⁷ C. W. Park,⁶²
 H. Park,³² S. Paul,⁶⁷ T. K. Pedlar,³⁶ L. Pesántez,³ R. Pestotnik,²⁴ M. Petrič,²⁴ L. E. Pilonen,⁷⁶ K. Prasanth,¹⁸
 C. Pulvermacher,²⁶ J. Rauch,⁶⁷ E. Ríbežl,²⁴ M. Ritter,³⁵ A. Rostomyan,⁸ S. Ryu,⁵⁹ H. Sahoo,¹⁴ Y. Sakai,^{15,12}
 S. Sandilya,⁶⁵ T. Sanuki,⁶⁹ Y. Sato,⁴² V. Savinov,⁵⁶ T. Schlüter,³⁵ O. Schneider,³³ G. Schnell,^{2,16} C. Schwanda,²¹
 A. J. Schwartz,⁷ Y. Seino,⁴⁹ K. Senyo,⁷⁸ O. Seon,⁴² I. S. Seong,¹⁴ V. Shebalin,^{4,51} T.-A. Shibata,⁷² J.-G. Shiu,⁴⁷
 B. Shwartz,^{4,51} F. Simon,^{38,66} J. B. Singh,⁵⁴ Y.-S. Sohn,⁷⁹ E. Solovieva,²³ S. Stanič,⁵⁰ M. Starič,²⁴ J. Stypula,⁴⁸
 M. Sumihama,¹¹ T. Sumiyoshi,⁷³ U. Tamponi,^{22,74} Y. Teramoto,⁵² M. Uchida,⁷² T. Uglov,^{23,41} S. Uno,^{15,12}
 P. Urquijo,³⁹ C. Van Hulse,² P. Vanhoefer,³⁸ G. Varner,¹⁴ K. E. Varvell,⁶³ A. Vinokurova,^{4,51} A. Vossen,¹⁹
 M. N. Wagner,¹⁰ C. H. Wang,⁴⁶ M.-Z. Wang,⁴⁷ X. L. Wang,⁷⁶ M. Watanabe,⁴⁹ Y. Watanabe,²⁵ K. M. Williams,⁷⁶
 E. Won,³⁰ J. Yelton,⁹ C. Z. Yuan,²⁰ Y. Yusa,⁴⁹ Z. P. Zhang,⁵⁸ V. Zhilich,^{4,51} V. Zhulanov,^{4,51} and A. Zupanc^{34,24}

(The Belle Collaboration)

¹Aligarh Muslim University, Aligarh 202002

²University of the Basque Country UPV/EHU, 48080 Bilbao

³University of Bonn, 53115 Bonn

⁴Budker Institute of Nuclear Physics SB RAS, Novosibirsk 630090

⁵Faculty of Mathematics and Physics, Charles University, 121 16 Prague

⁶Chonnam National University, Kwangju 660-701

⁷University of Cincinnati, Cincinnati, Ohio 45221

⁸Deutsches Elektronen-Synchrotron, 22607 Hamburg

⁹University of Florida, Gainesville, Florida 32611

¹⁰Justus-Liebig-Universität Gießen, 35392 Gießen

¹¹Gifu University, Gifu 501-1193

¹²SOKENDAI (The Graduate University for Advanced Studies), Hayama 240-0193

¹³Hanyang University, Seoul 133-791

¹⁴University of Hawaii, Honolulu, Hawaii 96822

¹⁵High Energy Accelerator Research Organization (KEK), Tsukuba 305-0801

¹⁶IKERBASQUE, Basque Foundation for Science, 48013 Bilbao

¹⁷Indian Institute of Technology Bhubaneswar, Satya Nagar 751007

¹⁸Indian Institute of Technology Madras, Chennai 600036

¹⁹Indiana University, Bloomington, Indiana 47408

²⁰Institute of High Energy Physics, Chinese Academy of Sciences, Beijing 100049

²¹Institute of High Energy Physics, Vienna 1050

²²INFN - Sezione di Torino, 10125 Torino

²³Institute for Theoretical and Experimental Physics, Moscow 117218

²⁴J. Stefan Institute, 1000 Ljubljana

²⁵Kanagawa University, Yokohama 221-8686

²⁶Institut für Experimentelle Kernphysik, Karlsruher Institut für Technologie, 76131 Karlsruhe

²⁷Kennesaw State University, Kennesaw GA 30144

²⁸King Abdulaziz City for Science and Technology, Riyadh 11442

²⁹Korea Institute of Science and Technology Information, Daejeon 305-806

- ³⁰ Korea University, Seoul 136-713
³¹ Kyoto University, Kyoto 606-8502
³² Kyungpook National University, Daegu 702-701
³³ École Polytechnique Fédérale de Lausanne (EPFL), Lausanne 1015
³⁴ Faculty of Mathematics and Physics, University of Ljubljana, 1000 Ljubljana
³⁵ Ludwig Maximilians University, 80539 Munich
³⁶ Luther College, Decorah, Iowa 52101
³⁷ University of Maribor, 2000 Maribor
³⁸ Max-Planck-Institut für Physik, 80805 München
³⁹ School of Physics, University of Melbourne, Victoria 3010
⁴⁰ Moscow Physical Engineering Institute, Moscow 115409
⁴¹ Moscow Institute of Physics and Technology, Moscow Region 141700
⁴² Graduate School of Science, Nagoya University, Nagoya 464-8602
⁴³ Kobayashi-Maskawa Institute, Nagoya University, Nagoya 464-8602
⁴⁴ Nara Women's University, Nara 630-8506
⁴⁵ National Central University, Chung-li 32054
⁴⁶ National United University, Miao Li 36003
⁴⁷ Department of Physics, National Taiwan University, Taipei 10617
⁴⁸ H. Niewodniczanski Institute of Nuclear Physics, Krakow 31-342
⁴⁹ Niigata University, Niigata 950-2181
⁵⁰ University of Nova Gorica, 5000 Nova Gorica
⁵¹ Novosibirsk State University, Novosibirsk 630090
⁵² Osaka City University, Osaka 558-8585
⁵³ Pacific Northwest National Laboratory, Richland, Washington 99352
⁵⁴ Panjab University, Chandigarh 160014
⁵⁵ Peking University, Beijing 100871
⁵⁶ University of Pittsburgh, Pittsburgh, Pennsylvania 15260
⁵⁷ Punjab Agricultural University, Ludhiana 141004
⁵⁸ University of Science and Technology of China, Hefei 230026
⁵⁹ Seoul National University, Seoul 151-742
⁶⁰ Soongsil University, Seoul 156-743
⁶¹ University of South Carolina, Columbia, South Carolina 29208
⁶² Sungkyunkwan University, Suwon 440-746
⁶³ School of Physics, University of Sydney, NSW 2006
⁶⁴ Department of Physics, Faculty of Science, University of Tabuk, Tabuk 71451
⁶⁵ Tata Institute of Fundamental Research, Mumbai 400005
⁶⁶ Excellence Cluster Universe, Technische Universität München, 85748 Garching
⁶⁷ Department of Physics, Technische Universität München, 85748 Garching
⁶⁸ Toho University, Funabashi 274-8510
⁶⁹ Department of Physics, Tohoku University, Sendai 980-8578
⁷⁰ Earthquake Research Institute, University of Tokyo, Tokyo 113-0032
⁷¹ Department of Physics, University of Tokyo, Tokyo 113-0033
⁷² Tokyo Institute of Technology, Tokyo 152-8550
⁷³ Tokyo Metropolitan University, Tokyo 192-0397
⁷⁴ University of Torino, 10124 Torino
⁷⁵ Utkal University, Bhubaneswar 751004
⁷⁶ CNP, Virginia Polytechnic Institute and State University, Blacksburg, Virginia 24061
⁷⁷ Wayne State University, Detroit, Michigan 48202
⁷⁸ Yamagata University, Yamagata 990-8560
⁷⁹ Yonsei University, Seoul 120-749

We search for the rare radiative decay $D^0 \rightarrow \gamma\gamma$ using a data sample with an integrated luminosity of 832 fb^{-1} recorded by the Belle detector at the KEKB e^+e^- asymmetric-energy collider. We find no statistically significant signal and set an upper limit on the branching fraction of $\mathcal{B}(D^0 \rightarrow \gamma\gamma) < 8.5 \times 10^{-7}$ at 90% confidence level. This is the most restrictive limit on the decay channel to date.

PACS numbers: 12.60.-i, 13.20.-v, 13.20.Fc, 13.25.Ft

Flavor-changing neutral current (FCNC) processes are forbidden at tree level in the standard model (SM), although they can occur at higher orders. In contrast, there are several new physics (NP) models that allow FCNC even at tree level and can substantially enhance

the branching fractions of the related decay processes. The decay of the neutral charm meson to two photons, $D^0 \rightarrow \gamma\gamma$, is one such example that constitutes a sensitive NP probe. Mediated by a $c \rightarrow u\gamma\gamma$ transition, the amplitude for this rare decay has very small [$\mathcal{O}(10^{-11})$]

short-distance contributions [1–3] due to the small size of the bottom-quark mass relative to the weak scale and a low value of the quark-mixing matrix [4] element V_{ub} . However, it is expected to have large long-distance contributions from intermediate vector mesons. Theory calculations based on vector meson dominance yield a decay branching fraction in the range $(1\text{--}3) \times 10^{-8}$ [2, 3, 5]. Using the framework of the minimal supersymmetric standard model (MSSM), the authors of Ref. [6] have predicted that the exchange of gluinos — the supersymmetric partners of gluons — can enhance the branching fraction up to 6×10^{-6} . Furthermore, it has been suggested that, by measuring $D^0 \rightarrow \gamma\gamma$, one would be able to better identify potential NP contributions to $D^0 \rightarrow \mu^+\mu^-$ [7].

Searches for the $D^0 \rightarrow \gamma\gamma$ decay have been previously conducted by the CLEO [8] and BABAR [9] experiments using e^+e^- collision data recorded at the $\Upsilon(4S)$ resonance and recently by BESIII [10] based on data collected near the open-charm threshold. The most stringent upper limit on the branching fraction is that set by BABAR: 2.2×10^{-6} at 90% confidence level (CL).

We report herein a search for $D^0 \rightarrow \gamma\gamma$ [11] using a data sample of 832 fb^{-1} collected near the $\Upsilon(4S)$ and $\Upsilon(5S)$ resonances with the Belle detector [12] at the KEKB asymmetric-energy e^+e^- collider [13]. The detector elements most relevant for the study are a tracking device comprising a silicon vertex detector and a central drift chamber (CDC); a particle identification system that consists of a barrel-like arrangement of time-of-flight counters (TOF) and an array of aerogel threshold Cherenkov counters (ACC); and a CsI(Tl) crystal-based electromagnetic calorimeter (ECL). All these components are located inside a superconducting solenoid coil that provides a 1.5 T magnetic field. In addition to data, we use Monte Carlo (MC) simulated events to devise selection criteria and study possible backgrounds. The relative size of the $\Upsilon(4S)$ and $\Upsilon(5S)$ MC samples is determined according to the integrated luminosity of the corresponding data.

To reduce large ‘combinatorial’ backgrounds arising from random photon combinations, we require that the D^0 be produced in the decay $D^{*+} \rightarrow D^0\pi^+$. The D^{*+} mesons mostly originate from the $e^+e^- \rightarrow c\bar{c}$ process via hadronization, where the inclusive yield has a large uncertainty of 12.5% [14]. To avoid this uncertainty, we measure the $D^0 \rightarrow \gamma\gamma$ branching fraction with respect to the well-measured mode $D^0 \rightarrow K_s^0\pi^0$ using the following relation:

$$\mathcal{B}(D^0 \rightarrow \gamma\gamma) = \frac{(N/\varepsilon)_{D^0 \rightarrow \gamma\gamma}}{(N/\varepsilon)_{D^0 \rightarrow K_s^0\pi^0}} \times \mathcal{B}(D^0 \rightarrow K_s^0\pi^0). \quad (1)$$

Here, N and ε are the signal yields and detection efficiencies, respectively, of the reconstructed channels and $\mathcal{B}(D^0 \rightarrow K_s^0\pi^0)$ is the world-average branching fraction for $D^0 \rightarrow K_s^0\pi^0$ [14]. Also, systematic uncertainties common to both the signal and normalization channels cancel in this measurement.

We identify photon candidates as localized energy deposits (“clusters”) in the ECL without any matched charged track in the CDC and having an energy greater than 200 MeV. Track candidates are required to have an impact parameter with respect to the interaction point (IP) of less than 1 cm in the transverse plane and less than 3 cm along the $+z$ axis (opposite the e^+ beam). Charged pions are distinguished from kaons [15] using specific ionization in the CDC, time-of-flight information from the TOF, and the number of photoelectrons from the ACC. The pion identification efficiency is above 95% while the probability to misidentify a kaon as a pion is below 5%. Candidate K_s^0 mesons are reconstructed from pairs of oppositely charged tracks (pion mass assumed) having a reconstructed mass within $9 \text{ MeV}/c^2$ of the nominal K_s^0 mass [14]. We reconstruct π^0 candidates from diphoton pairs with an invariant mass in the range $110\text{--}160 \text{ MeV}/c^2$. More details on the K_s^0 and π^0 reconstruction can be found in Ref. [16].

We reconstruct a D^0 candidate from two energetic photons. The D^0 candidate is then combined with a low-momentum (“slow”) pion, π_s^+ , to form a D^{*+} . We use two kinematic variables to identify signal: the reconstructed invariant mass of the D^0 candidate, $M(\gamma\gamma)$, and the difference between the reconstructed masses of the D^{*+} and D^0 candidates, ΔM . To improve the ΔM resolution, the π_s^+ track is constrained to originate from the IP. The D^0 candidate in the normalization channel is formed by combining a K_s^0 with a π^0 candidate. The signal peaks near the nominal D^0 mass [14] and at $145 \text{ MeV}/c^2$ in the $M(\gamma\gamma)$ and ΔM distributions, respectively. We select candidate events that satisfy the criteria $1.7 \text{ GeV}/c^2 < M(\gamma\gamma) < 2.0 \text{ GeV}/c^2$ and $140 \text{ MeV}/c^2 < \Delta M < 160 \text{ MeV}/c^2$. Furthermore, we define a smaller signal region as $1.711 \text{ GeV}/c^2 < M(\gamma\gamma) < 1.931 \text{ GeV}/c^2$ and $143.4 \text{ MeV}/c^2 < \Delta M < 147.7 \text{ MeV}/c^2$ [$\pm 3\sigma$ windows around the means of the $M(\gamma\gamma)$ and ΔM distributions], and a sideband as $1.95 \text{ GeV}/c^2 < M(\gamma\gamma) < 2.00 \text{ GeV}/c^2$ and $150 \text{ MeV}/c^2 < \Delta M < 160 \text{ MeV}/c^2$.

We study various backgrounds to the $D^0 \rightarrow \gamma\gamma$ signal. These can be broadly classified into three categories: peaking, QED, and combinatorial. The first is from specific physics processes such as $D^0 \rightarrow \pi^0\pi^0$, $D^0 \rightarrow \eta\pi^0$, $D^0 \rightarrow \eta\eta$, $D^0 \rightarrow K_s^0(\pi^0\pi^0)\pi^0$, and $D^0 \rightarrow K_L^0\pi^0$. These processes can be misidentified as signal in two different ways. One possibility is from a pair of high-energy photons, either one or both coming from a π^0 or η decay. This is suppressed by pairing each photon candidate of $D^0 \rightarrow \gamma\gamma$ with all other photons in the event and applying criteria on the resulting probabilities, $\mathcal{P}(\pi^0)$ and $\mathcal{P}(\eta)$ [17]. The second possibility is due to merged clusters in the ECL owing to a small opening angle between two photons from a high-momentum π^0 or η decay. Such clusters are wider in the lateral dimension and are rejected by requiring that the energy deposited in the 3×3 array of crystals centered on the crystal with the highest energy exceeds 85% of the energy deposited in the corresponding 5×5 array of crystals. In the case of

$D^0 \rightarrow K_L^0 \pi^0$, misidentification of the K_L^0 as a γ candidate contributes to the background. The peaking background exhibits a signal-like peak in the ΔM distribution but peaks at a lower $M(\gamma\gamma)$ value due to particles missing from the reconstruction.

The QED background arises from out-of-time $e^+e^- \rightarrow \gamma\gamma$ and $e^+e^- \rightarrow e^+e^-(\gamma)$ events. To suppress its contribution, we retain only those events in which the number of charged tracks and photon candidates each exceeds four. We also require the timing of ECL clusters for photon candidates to lie within a $2\mu\text{sec}$ window around the beam collision time identified at the trigger level. With these criteria, we find a negligible contribution from the QED background (3% of the total background).

To suppress remaining backgrounds, we apply selection requirements on the following variables: the momentum of the D^* candidate in the e^+e^- center-of-mass frame, $p^*(D^*)$; the energy asymmetry between the two photons, $A_E = (E_{\gamma 1} - E_{\gamma 2}) / (E_{\gamma 1} + E_{\gamma 2})$, where $E_{\gamma 1(2)}$ is the energy of the higher (lower) energy photon; $E_{\gamma 2}$; $\mathcal{P}(\pi^0)$; and $\mathcal{P}(\eta)$. The requirements are determined using an optimization procedure [18] with a figure-of-merit given by

$$\text{FOM} = \frac{\varepsilon(t)}{\sqrt{N_B(t)}}, \quad (2)$$

where t is the value of the selection criterion and ε and N_B are, respectively, the detection efficiency and the number of background events expected in the signal region. As the contribution of $\sqrt{N_B(t)}$ is overwhelming, we neglect the $a/2$ term in the denominator of the original FOM expression in Ref. [18], where a is the desired CL in terms of standard deviations. We use signal MC events to estimate ε and a blended MC sample of $e^+e^- \rightarrow q\bar{q}$ ($q = u, d, s, c$) and $B\bar{B}$ events to calculate N_B . Some of the variables, notably $E_{\gamma 2}$ and A_E , can have significant correlations among themselves. We take this effect into account via simultaneous optimizations of the criteria in these variables.

To incorporate possible differences between data and simulations in the optimization procedure, we multiply N_B in Eq. (2) by a correction factor estimated by comparing data and MC events in the sideband. The factor could be as large as 1.6, depending on the variable. The selection criteria obtained are $p^*(D^*) > 2.9\text{ GeV}/c$, $E_{\gamma 2} > 900\text{ MeV}$, $A_E < 0.5$, $\mathcal{P}(\pi^0) < 0.15$, and no requirement on $\mathcal{P}(\eta)$. We have verified that the same set of criteria can be applied to the combined sample of $\Upsilon(4S)$ and $\Upsilon(5S)$ data with the level of backgrounds being proportional to the respective luminosity.

The efficiency for signal events to pass the above selection criteria is $(7.34 \pm 0.05)\%$. About 3% of the events selected in the signal MC sample have multiple D^{*+} candidates. In these cases, we retain the one with the smallest value of the π_s^+ impact parameter with respect to the IP in the transverse plane. If there is a unique π_s^+ but multiple D^0 candidates, the first one is arbitrarily chosen.

From simulations, we find that this criterion identifies the correct D^{*+} decay in 70% of the cases.

Event candidates for the normalization channel $D^0 \rightarrow K_s^0 \pi^0$ are selected with criteria similar to those of the signal for π_s^+ , $p^*(D^*)$, ΔM , and the invariant mass of the D^0 candidate. For the criteria that differ from those of the signal selection, we rely on Ref. [16]. With these requirements, the detection efficiency is found to be $(7.18 \pm 0.05)\%$.

To extract the signal yield, we perform an unbinned extended maximum likelihood fit to the two-dimensional (2D) distributions of $M(\gamma\gamma)$ and ΔM . For the signal and combinatorial-background component, the correlation between the two observables is negligible. Thus we define a combined probability density function (PDF) for each component, indexed by j , as

$$\mathcal{P}_j \equiv \mathcal{P}_j[M(\gamma\gamma)] \mathcal{P}_j[\Delta M]. \quad (3)$$

The signal shape in both $M(\gamma\gamma)$ and ΔM is described by a sum of a Gaussian and an asymmetric Gaussian function of common mean. The combinatorial background shape in $M(\gamma\gamma)$ is modeled by a third-order polynomial and in ΔM by a threshold function $(x - m_{\pi^+})^\alpha \exp[-\beta(x - m_{\pi^+})]$, where α and β are two shape parameters and m_{π^+} is the nominal charged pion mass [14]. For the peaking background, there is a significant correlation between ΔM and $M(\gamma\gamma)$, which we account for via a joint PDF $\mathcal{P}[\Delta M|M(\gamma\gamma)]$. This background component is described by a single Gaussian function in $M(\gamma\gamma)$ and, just as for the signal, the sum of a Gaussian and an asymmetric Gaussian function in ΔM . To include the correlation, we parametrize the width of the Gaussian part of ΔM as $\sigma = \sigma_0(1 + k[M(\gamma\gamma) - m_{D^0}]^2)$, where σ_0 is the uncorrelated value, k is the correlation coefficient, and m_{D^0} is the world-average D^0 mass [14]. The two widths of the asymmetric Gaussian component are scaled from σ . All combinatorial PDF parameters are determined from the data fit, while those for signal and peaking background are fixed to the corresponding MC values.

To take possible data–MC difference into account for the signal PDFs, we use a sample of $D^0 \rightarrow \phi(K^+K^-)\gamma$, from which we extract the shift in mean values and the ratio of widths between data and simulations as calibration factors. The control mode suffers from significant contamination from $D^0 \rightarrow \phi(K^+K^-)\pi^0$. To better discriminate signal from this background, we include the helicity angle in the fit, which is defined as the angle between the K^+ momentum and the negative of the D^0 momentum in the ϕ rest frame. As we wish to apply correction factors obtained from $D^0 \rightarrow \phi\gamma$, which contains one photon, to the signal channel with two photons in the final state, we shift the MC $M(\gamma\gamma)$ mean value by twice its correction and multiply the width by the square of the corresponding correction factor. On the other hand, the ΔM resolution is dominated by the momentum measurement of π_s^+ , for which there is no difference between

the signal and control channel. Therefore, the ΔM corrections are applied without any change.

To calibrate the peaking background shape in $M(\gamma\gamma)$, we compare data and MC distributions in a sample of $D^0 \rightarrow \pi^0\pi^0$ that is partially reconstructed using the higher-energy photons from each π^0 decay. The ΔM correction factors are obtained using a sample of candidates in data and MC events for the forbidden decay $D^0 \rightarrow K_s^0\gamma$, where the selected candidates are mostly due to partially reconstructed $D^0 \rightarrow K_s^0\pi^0$ decays.

We apply the fit to simulated MC samples and obtain yields for the three event categories that are consistent with their input values. Furthermore, we check the stability and error coverage of the fit by applying it to an ensemble of pseudo-experiments where events are drawn from the PDF shapes for all three event categories as described above. The exercise is repeated for various possible signal yields ranging from 0 to 100. We find a negligible bias on the fitted signal yield and the latter consistent with the input value within uncertainties.

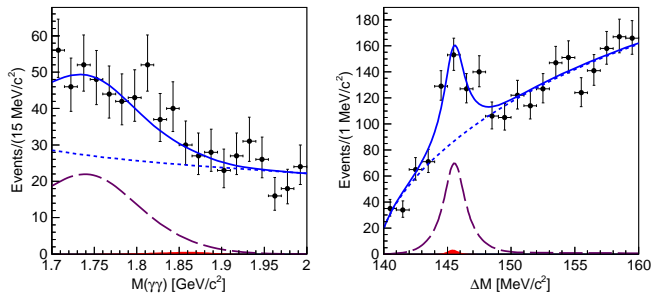


FIG. 1. Projections of candidate events onto the $M(\gamma\gamma)$ (left) and ΔM (right) distributions, applying a signal-region criterion on the other variable. Points with error bars are the data, blue solid curves are the results of the fit, blue dotted curves represent the combinatorial background, magenta dashed curves are the peaking background, and red filled histograms show the signal component.

Applying the 2D fit described above to the 3148 candidate events, we find 4 ± 15 signal, 210 ± 32 peaking background and 2934 ± 59 combinatorial background events. Figure 1 shows the results of the fit. The peaking background in the $M(\gamma\gamma)$ plot is predominantly due to the $D^0 \rightarrow \pi^0\pi^0$ decay; the yield of this background is consistent with the MC expectation. The χ^2/NDF for the two fit projections are 0.68 and 1.09, respectively, which indicate that the fit gives a good description of the data.

In the absence of a statistically significant signal, we derive an upper limit at 90% CL on the signal yield ($N_{\text{UL}}^{90\%}$) following a frequentist method [19] using an ensemble of pseudo-experiments. For a given signal yield, we generate 5000 sets of signal and background events according to their PDFs, and perform the fit. The CL is obtained by calculating the fraction of samples that gives a fit yield larger than that observed in data (4

events). The systematic uncertainty (described below) is accounted for in the limit calculation by smearing the fit yield. We obtain $N_{\text{UL}}^{90\%}$ to be 25 events.

As this is a relative measurement, most of the systematic uncertainties common between the signal and normalization channels cancel. However, some residual systematics remain. We estimate their contributions by varying the selection criteria that do not necessarily factor out. These include $E_{\gamma 2}$, A_E , and $\mathcal{P}(\pi^0)$. For $E_{\gamma 2}$ we estimate N/ε with and without any requirement on the photon energy in the $D^0 \rightarrow \phi\gamma$ control sample. The change with respect to the nominal value is taken as the corresponding systematic error. The uncertainty due to the $\mathcal{P}(\pi^0)$ requirement is calculated in the same control sample by comparing the nominal yield with the one obtained with a substantially relaxed criterion [$\mathcal{P}(\pi^0) < 0.7$]. We double the above systematic uncertainties, as our signal has two photons. Since we do not have a proper control sample for A_E , we fit to the data without this requirement and take the resulting change in the upper limit as the systematic error.

Another source of systematics is due to the calibration factors applied to MC-determined PDF shapes for the fit to data. In case of signal, we repeat the fit by varying the PDF shapes in accordance with the uncertainties obtained in the $D^0 \rightarrow \phi\gamma$ control channel and take the change in the signal yield as the systematic error. To estimate the PDF shape uncertainty due to the peaking background, similar exercises are also performed by changing the corresponding calibration factors by $\pm 1\sigma$.

Finally, there is a systematic uncertainty in the efficiencies for photon detection, K_s^0 , and π^0 reconstruction. The systematic error due to photon detection is about 2.2% for $E_\gamma = 1$ GeV [20]. With two energetic photons in the signal final state, we assign a 4.4% uncertainty. The uncertainty associated with K_s^0 reconstruction is estimated with a sample of $D^{*+} \rightarrow D^0\pi_s^+$, $D^0 \rightarrow K_s^0(\pi^+\pi^-)\pi^+\pi^-$ decays and is 0.7%. We obtain the systematic error due to π^0 reconstruction (4.0%) by comparing data-MC differences of the yield ratio between $\eta \rightarrow \pi^0\pi^0\pi^0$ and $\eta \rightarrow \pi^+\pi^-\pi^0$. The last error is that on the branching fraction of the normalization channel $D^0 \rightarrow K_s^0\pi^0$ [14]. Table I summarizes all systematic sources along with their contributions.

The 2D fit is then applied to the normalization channel of $D^0 \rightarrow K_s^0\pi^0$, using the same signal and background models as for $D^0 \rightarrow \gamma\gamma$. All signal shape parameters are floated during the fit. We find a signal yield of $343\,050 \pm 673$ events. Using the above information in Eq. (1), we obtain a 90% CL upper limit on the branching fraction of $\mathcal{B}(D^0 \rightarrow \gamma\gamma) < 8.5 \times 10^{-7}$. In Fig. 2, we compare our upper limit with those obtained by CLEO, BESIII and BABAR as well as with the $c \rightarrow u\gamma$ branching fractions expected in the SM and MSSM [5].

In summary, we search for the rare decay $D^0 \rightarrow \gamma\gamma$ using the full data sample recorded by the Belle experiment at or above the $\Upsilon(4S)$ resonance. In the absence of a statistically significant signal, a 90% CL upper

TABLE I. Summary of systematic uncertainties for $D^0 \rightarrow \gamma\gamma$.

Source	Contribution
Cut variation	$\pm 6.8\%$
PDF shape	$+4.0$ -2.4 events
Photon detection	$\pm 4.4\%$
K_S^0 reconstruction	$\pm 0.7\%$
π^0 identification	$\pm 4.0\%$
$\mathcal{B}(D^0 \rightarrow K_S^0 \pi^0)$	$\pm 3.3\%$

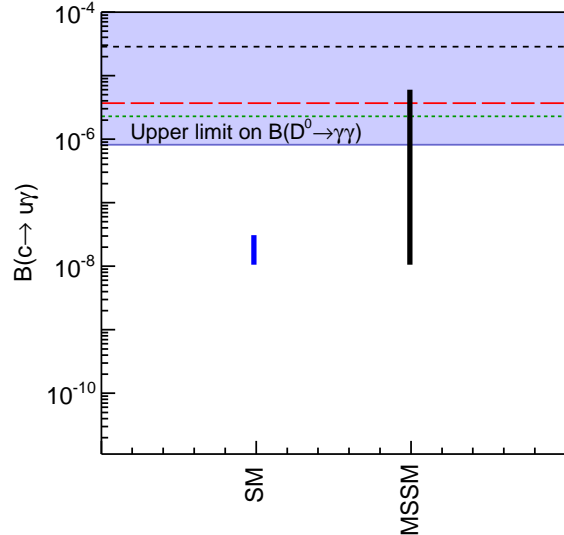


FIG. 2. Ranges of the $c \rightarrow u\gamma$ branching fraction predicted in the SM and MSSM [5] are compared with our obtained upper limit on $\mathcal{B}(D^0 \rightarrow \gamma\gamma)$, shown by the purple solid line. The limits from *BABAR* [9], *BESIII* [10], and *CLEO* [8] are indicated by the green dotted, red long-dashed, and black dashed lines, respectively.

limit is set on its branching fraction of 8.5×10^{-7} . Our result constitutes the most restrictive limit on $D^0 \rightarrow \gamma\gamma$ to date and can be used to constrain NP parameter spaces. This FCNC decay will be probed further at the next-generation Belle II experiment [21].

We thank the KEKB group for excellent operation of the accelerator; the KEK cryogenics group for efficient solenoid operations; and the KEK computer group, the NII, and PNNL/EMSL for valuable computing and SINET4 network support. We acknowledge support from MEXT, JSPS and Nagoya's TLPRC (Japan); ARC (Australia); FWF (Austria); NSFC and CCEPP (China); MSMT (Czechia); CZE, DFG, and VS (Germany); DST (India); INFN (Italy); MOE, MSIP, NRF, BK21Plus, WCU and RSRI (Korea); MNiSW and NCN (Poland); MES and RFAAE (Russia); ARRS (Slovenia); IKER-BASQUE and UPV/EHU (Spain); SNSF (Switzerland); NSC and MOE (Taiwan); and DOE and NSF (USA).

[1] C. Greub, T. Hurth, M. Misiak, and D. Wyler, *Phys. Lett. B* **382**, 415 (1996).
[2] S. Fajfer, P. Singer, and J. Zupan, *Phys. Rev. D* **64**, 074008 (2001).
[3] G. Burdman, E. Golowich, J. A. Hewett, and S. Pakvasa, *Phys. Rev. D* **66**, 014009 (2002).

[4] N. Cabibbo, *Phys. Rev. Lett.* **10**, 531 (1963); M. Kobayashi and T. Maskawa, *Prog. Theor. Phys.* **49**, 652 (1973).
[5] S. W. Bosch and G. Buchalla, *JHEP* **0208**, 054 (2002).
[6] S. Prelovsek and D. Wyler, *Phys. Lett. B* **500**, 304 (2001).

- [7] A. Paul, I. I. Bigi, and S. Recksiegel, *Phys. Rev. D* **82**, 094006 (2010).
- [8] T. E. Coan *et al.* (CLEO Collaboration), *Phys. Rev. Lett.* **90**, 101801 (2003).
- [9] J. P. Lees *et al.* (BABAR Collaboration), *Phys. Rev. D* **85**, 091107 (2012).
- [10] M. Ablikim *et al.* (BESIII Collaboration), *Phys. Rev. D* **91**, 112015 (2015).
- [11] Throughout this paper, the charge-conjugate decay modes are always implied unless stated otherwise.
- [12] A. Abashian *et al.* (Belle Collaboration), *Nucl. Instrum. Methods Phys. Res., Sect. A* **479**, 117 (2002); also, see the detector section in J. Brodzicka *et al.*, *Prog. Theor. Exp. Phys.*, 04D001 (2012).
- [13] S. Kurokawa and E. Kikutani, *Nucl. Instrum. Methods Phys. Res., Sect. A* **499**, 1 (2003), and other papers in this volume; T. Abe *et al.*, *Prog. Theor. Exp. Phys.*, 03A001 (2013) and following articles up to 03A011.
- [14] K. A. Olive *et al.* (Particle Data Group), *Chin. Phys. C* **38**, 090001 (2014).
- [15] E. Nakano, *Nucl. Instrum. Methods Phys. Res., Sect. A* **494**, 402 (2002).
- [16] N. K. Nisar *et al.* (Belle Collaboration), *Phys. Rev. Lett.* **112**, 211601 (2014).
- [17] P. Koppenburg *et al.* (Belle Collaboration), *Phys. Rev. Lett.* **93**, 061803 (2004).
- [18] G. Punzi, *eConf C* **030908** (2003) MODT022 [arXiv:physics/0308063].
- [19] Y. Liu *et al.* (Belle Collaboration), *Phys. Rev. D* **78**, 011106 (2008).
- [20] D. Dutta *et al.* (Belle Collaboration), *Phys. Rev. D* **91**, 011101(R) (2015).
- [21] T. Abe *et al.* (Belle II Collaboration), arXiv:1011.0352 [physics.ins-det].